INTERNATIONAL JOURNAL FOR NUMERICAL METHODS IN FLUIDS, VOL. 24, 759–769 (1997)

TRANSIENT SIMULATION OF INTERNAL SEPARATED FLOWS USING AN INTELLIGENT HIGHER-ORDER SPATIAL DISCRETIZATION SCHEME

OLCAY OYMAK AND NEVİN SELÇUK

Department of Chemical Engineering, Middle East Technical University, 06531 Ankara, Turkey

SUMMARY

This paper summarizes the method-of-lines (MOL) solution of the Navier–Stokes equations for an impulsively started incompressible laminar flow in a circular pipe with a sudden expansion. An intelligent higher-order spatial discretization scheme, which chooses upwind or downwind discretization in a zone-of-dependence manner when flow reversal occurs, was developed for separated flows. Stability characteristics of a linear advective–diffusive equation were examined to depict the necessity of such a scheme in the case of flow reversals. The proposed code was applied to predict the time development of an impulsively started flow in a pipe with a sudden expansion. Predictions were found to show the expected trends for both unsteady and steady states. This paper demonstrates the ease with which the Navier–Stokes equations can be solved in an accurate manner using sophisticated numerical algorithms for the solution of ordinary differential equations (ODEs). Solutions of the Navier–Stokes equations in primitive variables formulation by using the MOL and intelligent higher-order spatial discretization scheme are not available to date. © 1997 by John Wiley & Sons, Ltd.

KEY WORDS: computational fluid dynamics; method of lines; internal separated flows; higher-order spatial discretization

1. INTRODUCTION

In the field of computational fluid dynamics (CFD) the advent of computers with their constantly growing processing and storing capabilities has made it possible to compute very complex flow fields by the numerical solution of the Navier–Stokes equations. Several computational schemes have been proposed for both steady and unsteady formulations. Most of these numerical techniques are based on finite difference,[1,2] finite element[2–5] or finite volume methods.[6] However, in order to investigate the detailed unsteady structures of a flow field, a more accurate and efficient method, which this paper introduces, is still needed.

Conventional algorithms for the solution of PDEs consist of approximating the spatial derivatives and temporal derivatives separately. The method proposed in this paper is another numerical technique for the solution of partial differential equations (PDEs). The proposed technique, the MOL, consists of two stages. In the first stage the PDE system is converted into an ODE initial value problem by discretizing the spatial derivatives, together with the boundary conditions, via Taylor series, spline or weighted residual techniques, while in the second stage the resulting ODEs are integrated using a sophisticated ODE solver which takes the burden of time discretization and chooses the time steps in a way that maintains the accuracy and stability of the evolving solution.

CCC 0271–2091/97/080759–11 $17.50

Received November 1995
Revised April 1996

Therefore many existing numerical algorithms for transient PDEs can be considered as MOL algorithms. The most important advantage of the MOL approach is that it combines the simplicity of the explicit method with the superiority of the implicit ones unless a poor numerical method for the solution of ODEs is used. The computational accuracy and efficiency of this method have previously been reported by the present authors.[7] However, when flow reversal occurs, inappropriate discretization of the advective terms in the Navier–Stokes equations leads to an unstable ODE problem for both conventional and MOL algorithms. This bottleneck can be alleviated naturally by tailoring an intelligent scheme which employs directional differentiation when the flow field has recirculation zones.

For convection-dominated flows the use of centred difference formulae for the convective terms leads to solutions with severe non-physical oscillations. Since the beginning of CFD studies, attempts have been made to stabilize the flow solution by discretizing the convective terms in two-point upwind difference expressions. However, the well-known drawback of this discretization is its first-order accuracy. Therefore solutions with the use of first-order-accurate upwind discretizations are generally inaccurate, particularly if the local velocity gradients are large. More accurate solutions are obtained if the convective terms are represented by higher-order upwind schemes.

In the present paper the primitive variables formulation is used for solving the two-dimensional, unsteady Navier–Stokes equations for an impulsively started flow in a circular pipe with a sudden expansion. In the spatial discretization scheme, where the five-point Lagrange interpolation polynomial is used, convective terms are discretized by assigning a direction to the differentiation scheme according to the sign of the velocity components, while diffusive terms are discretized centrally. The structured grid generator based on quadrilateral serendipity elements is used.

The main contribution of this paper is to propose a Navier–Stokes code based on the MOL approach with an intelligent higher-order spatial discretization scheme which decides whether to use upwind or downwind discretization in a zone-of-dependence manner for the approximation of the advective terms when flow reversal occurs.

2. GOVERNING EQUATIONS

The flow to be studied in this paper is assumed to be a laminar, two-dimensional, unsteady and incompressible developing flow in a circular duct with a sudden expansion. With these assumptions the Navier–Stokes equations and continuity equation can be written as

$$\frac{\partial u}{\partial t} = -u\frac{\partial u}{\partial z} - v\frac{\partial u}{\partial r} - \frac{1}{\rho}\frac{\partial p}{\partial z} + \nu\left(\frac{\partial^2 u}{\partial z^2} + \frac{1}{r}\frac{\partial u}{\partial r} + \frac{\partial^2 u}{\partial r^2}\right), \tag{1}$$

$$\frac{\partial v}{\partial t} = -u\frac{\partial v}{\partial z} - v\frac{\partial v}{\partial r} - \frac{1}{\rho}\frac{\partial p}{\partial r} + \nu\left(\frac{\partial^2 v}{\partial z^2} + \frac{1}{r}\frac{\partial v}{\partial r} + \frac{\partial^2 v}{\partial r^2} - \frac{v}{r^2}\right), \tag{2}$$

$$\frac{\partial u}{\partial z} + \frac{\partial v}{\partial r} + \frac{v}{r} = 0, \tag{3}$$

where u and v represent the axial (z) and radial (r) components of the velocity, p is the static pressure, ν is the kinematic viscosity and t is the time.

2.1. Initial and boundary conditions

The geometry under consideration in this study is a circular pipe with a sudden expansion. As can be seen from Figure 1, the boundary conditions for the axial and radial components of the velocity vector are as follows. At the inlet the axial component of the velocity is given by a parabolic profile and the radial component is set to zero. At the outlet the boundary conditions are given by setting the second derivatives of the components of the velocity vector to zero ($\partial^2 u/\partial z^2 = 0$, $\partial^2 v/\partial z^2 = 0$). At the walls the components of the velocity vector vanish. At the centreline the symmetry condition is imposed for the axial component of the velocity and the radial component is set to zero.

The sudden start of the flow at the beginning of the time ($t = 0$) prescribe a zero velocity field in the entire computational domain, except at the inlet of the pipe where a certain mass flux with a parabolic velocity profile is set.

3. APPLICATION OF THE MOL

In the MOL approach the first stage in the solution of the Navier–Stokes equations is to discretize the spatial derivatives and the second stage is to integrate the resulting system of ODEs by a powerful ODE solver.

In the application of the first stage the convective derivatives should be approximated in such a way that the resulting system of ODEs is stable according to the linear theory.[8] What is meant by stability is that the real parts of the eigenvalues of the system of ODEs should be negative. This can only be achieved by using an intelligent spatial discretization scheme which is based on the choice of upwind or downwind points for the approximation of the convective derivatives. In the proposed study an intelligent higher-order spatial discretization scheme based on the five-point Lagrange interpolation polynomial is used not only to ensure stability but also to satisfy accuracy. After satisfaction of the stability of the problem an implicit time integration method should be applied to warrant the stability of the numerical integration of ODEs. Here the stability of the ODE problem should not be confused with the stability of the numerical integration. Details about the ODE problem stability and the stability of numerical integration can be found elsewhere.[8]

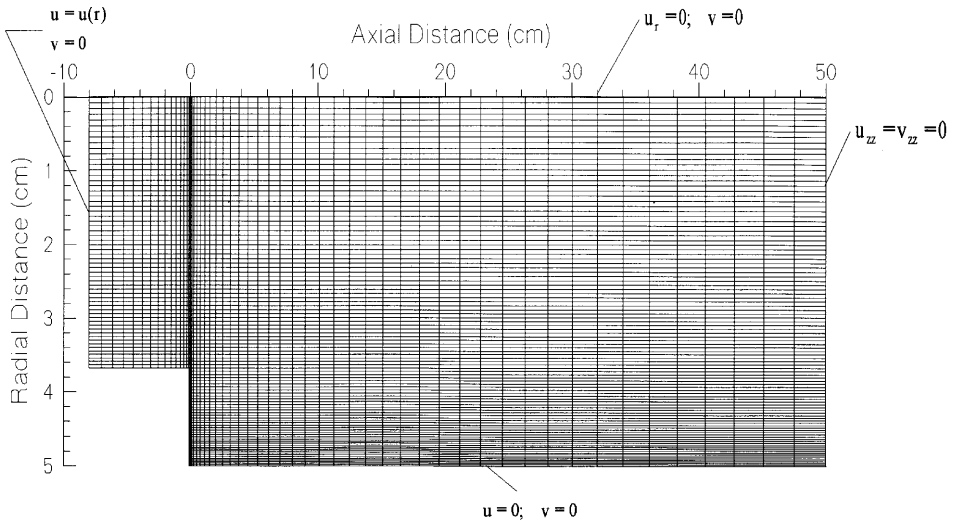

Figure 1. Flow geometry, computational domain and boundary conditions

4. STABILITY ANALYSIS

The problem stability is illustrated on the numerical solution of a generic convective–diffusive equation which can be written in non-conservative form as

$$\frac{\partial\phi}{\partial t}+\bar{u}\frac{\partial\phi}{\partial x}+\bar{v}\frac{\partial\phi}{\partial y}=\Gamma\left(\frac{\partial^2\phi}{\partial x^2}+\frac{\partial^2\phi}{\partial y^2}\right), \tag{4}$$

where ϕ is the dependent property, $\bar{u}$ is the x-component velocity, $\bar{v}$ is the y-component velocity and Γ is the diffusivity. Let the boundary conditions for the dependent property ϕ be time-independent Dirichlet-type conditions on the boundaries of the physical domain. Discretization of the spatial derivatives of equation (4) with different schemes is carried out as follows. For the sake of simplicity the discretization of the convective derivatives for the upwind and downwind cases is carried out by a first-order-accurate scheme, whereas that of the diffusive and convective derivatives for the centred case is performed by a second-order-accurate scheme.

4.1. Upwind discretization

$$\frac{\mathrm{d}\phi_{i,j}}{\mathrm{d}t}+\frac{\bar{u}}{\Delta x}(\phi_{i,j}-\phi_{i-1,j})+\frac{\bar{v}}{\Delta y}(\phi_{i,j}-\phi_{i,j-1})=\frac{\Gamma}{\Delta x^2}(\phi_{i+1,j}-2\phi_{i,j}+\phi_{i-1,j})+\frac{\Gamma}{\Delta y^2}(\phi_{i,j+1}-2\phi_{i,j}+\phi_{i,j-1}), \tag{5a}$$

$$\frac{\mathrm{d}\phi_{i,j}}{\mathrm{d}t}=\underbrace{\left(\frac{\bar{u}}{\Delta x}+\frac{\Gamma}{\Delta x^2}\right)}_{A}\phi_{i-1,j}+\underbrace{\left(-\frac{\bar{u}}{\Delta x}-\frac{\bar{v}}{\Delta y}-\frac{2\Gamma}{\Delta x^2}-\frac{2\Gamma}{\Delta y^2}\right)}_{B}\phi_{i,j}+\underbrace{\left(\frac{\Gamma}{\Delta x^2}\right)}_{C}\phi_{i+1,j}+\underbrace{\left(\frac{\bar{v}}{\Delta y}+\frac{\Gamma}{\Delta y^2}\right)}_{D}\phi_{i,j-1}+\underbrace{\left(\frac{\Gamma}{\Delta y^2}\right)}_{E}\phi_{i,j+1}. \tag{5b}$$

4.2. Downwind discretization

$$\frac{\mathrm{d}\phi_{i,j}}{\mathrm{d}t}+\frac{\bar{u}}{\Delta x}(\phi_{i+1,j}-\phi_{i,j})+\frac{\bar{v}}{\Delta y}(\phi_{i,j+1}-\phi_{i,j})=\frac{\Gamma}{\Delta x^2}(\phi_{i+1,j}-2\phi_{i,j}+\phi_{i-1,j})+\frac{\Gamma}{\Delta y^2}(\phi_{i,j+1}-2\phi_{i,j}+\phi_{i,j-1}), \tag{6a}$$

$$\frac{\mathrm{d}\phi_{i,j}}{\mathrm{d}t}=\underbrace{\left(\frac{\Gamma}{\Delta x^2}\right)}_{A}\phi_{i-1,j}+\underbrace{\left(\frac{\bar{u}}{\Delta x}+\frac{\bar{v}}{\Delta y}-\frac{2\Gamma}{\Delta x^2}-\frac{2\Gamma}{\Delta y^2}\right)}_{B}\phi_{i,j}+\underbrace{\left(-\frac{\bar{u}}{\Delta x}+\frac{\Gamma}{\Delta x^2}\right)}_{C}\phi_{i+1,j}+\underbrace{\left(\frac{\Gamma}{\Delta y^2}\right)}_{D}\phi_{i,j-1}+\underbrace{\left(-\frac{\bar{v}}{\Delta y}+\frac{\Gamma}{\Delta y^2}\right)}_{E}\phi_{i,j+1}. \tag{6b}$$

4.3. Centred discretization

$$\frac{\mathrm{d}\phi_{i,j}}{\mathrm{d}t}+\frac{\bar{u}}{2\Delta x}(\phi_{i+1,j}-\phi_{i-1,j})+\frac{\bar{v}}{2\Delta y}(\phi_{i,j+1}-\phi_{i,j-1})=\frac{\Gamma}{\Delta x^2}(\phi_{i+1,j}-2\phi_{i,j}+\phi_{i-1,j})+\frac{\Gamma}{\Delta y^2}(\phi_{i,j+1}-2\phi_{i,j}+\phi_{i,j-1}), \quad (7a)$$

$$\frac{\mathrm{d}\phi_{i,j}}{\mathrm{d}t}=\underbrace{\left(\frac{\bar{u}}{2\Delta x}+\frac{\Gamma}{\Delta x^2}\right)}_{A}\phi_{i-1,j}+\underbrace{\left(-\frac{2\Gamma}{\Delta x^2}-\frac{2\Gamma}{\Delta y^2}\right)}_{B}\phi_{i,j}+\underbrace{\left(-\frac{\bar{u}}{2\Delta x}+\frac{\Gamma}{\Delta x^2}\right)}_{C}\phi_{i+1,j}+\underbrace{\left(\frac{\bar{v}}{2\Delta y}+\frac{\Gamma}{\Delta y^2}\right)}_{D}\phi_{i,j-1}+\underbrace{\left(-\frac{\bar{v}}{2\Delta y}+\frac{\Gamma}{\Delta y^2}\right)}_{E}\phi_{i,j+1}. \quad (7b)$$

The system of ODEs resulting from equations (5)–(7) can be expressed as

$$\frac{\mathrm{d}\phi_{i,j}}{\mathrm{d}t}=A\phi_{i-1,j}+B\phi_{i,j}+C\phi_{i+1,j}+D\phi_{i,j-1}+E_{i,j+1}. \quad (8)$$

The coefficients A, B, C, D and E for different discretization schemes are summarized in terms of mesh Peclet numbers ($Pe_x=\bar{u}\Delta x/\Gamma, Pe_y=\bar{v}\Delta y/\Gamma$) in Table I.

The solution of equation (8) for the particular scheme illustrated in Figure 2 by the MOL approach, whatever the discretization scheme is, results in a system of linear ODEs which can be expressed in matrix form as

$$\frac{\mathrm{d}\bar{\Phi}}{\mathrm{d}t}=[P]\bar{\Phi}+\bar{Q}, \quad (9)$$

Table I. Summary of coefficients *A*, *B*, *C*, *D* and *E* with respect to different schemes

	Upwind scheme	Downwind scheme	Centred scheme
A	$\frac{\Gamma}{\Delta x^2}(1+Pe_x)$	$\frac{\Gamma}{\Delta x^2}$	$\frac{\Gamma}{\Delta x^2}\left(1+\frac{Pe_x}{2}\right)$
B	$-\frac{\Gamma}{\Delta x^2}(Pe_x+2)-\frac{\Gamma}{\Delta y^2}(Pe_y+2)$	$\frac{\Gamma}{\Delta x^2}(Pe_x-2)+\frac{\Gamma}{\Delta y^2}(Pe_y-2)$	$-2\left(\frac{\Gamma}{\Delta x^2}+\frac{\Gamma}{\Delta y^2}\right)$
C	$\frac{\Gamma}{\Delta x^2}$	$\frac{\Gamma}{\Delta x^2}(1-Pe_x)$	$\frac{\Gamma}{\Delta x^2}\left(1-\frac{Pe_x}{2}\right)$
D	$\frac{\Gamma}{\Delta y^2}(1+Pe_y)$	$\frac{\Gamma}{\Delta y^2}$	$\frac{\Gamma}{\Delta y^2}\left(1+\frac{Pe_y}{2}\right)$
E	$\frac{\Gamma}{\Delta y^2}$	$\frac{\Gamma}{\Delta y^2}(1-Pe_y)$	$\frac{\Gamma}{\Delta y^2}\left(1-\frac{Pe_y}{2}\right)$

where $\bar{\Phi}$ is a vector of dependent variables, $[P]$ is the Jacobian matrix and $\bar{Q}$ is a vector accounting for the time-independent Dirichlet boundary conditions. The components of $\bar{\Phi}$, $[P]$ and $\bar{Q}$ in terms of the quantities in Table I are

$$\bar{\Phi} = \begin{bmatrix} \phi_1 \\ \phi_2 \\ \phi_3 \\ \phi_4 \end{bmatrix}, \qquad [P] = \begin{bmatrix} B & E & 0 & C \\ D & B & C & 0 \\ 0 & A & B & D \\ A & 0 & E & B \end{bmatrix}, \qquad \bar{Q} = \begin{bmatrix} A\phi_8 + D\phi_6 \\ A\phi_9 + E\phi_{11} \\ C\phi_{14} + E\phi_{12} \\ C\phi_{15} + D\phi_5 \end{bmatrix}.$$

The general solution of equation (9), which is a non-homogeneous linear equation, can be expressed as

$$\bar{\Phi} = \bar{\Phi}_{\mathrm{h}} + \bar{\Phi}_{\mathrm{p}}, \tag{10}$$

where $\bar{\Phi}_{\mathrm{h}}$ is the solution of the corresponding homogeneous equation and $\bar{\Phi}_{\mathrm{p}}$ is the particular solution of the non-homogeneous equation. Hence the general solution of equation (9) can be written as

$$\Phi_i = \sum_{j=1}^{4} C_{i,j} \mathrm{e}^{\lambda_j t} + \Phi_{\mathrm{p}_i}, \quad i = 1, \ldots, 4 \tag{11}$$

where the Cs are eigenvectors and the λs are the eigenvalues. According to the linear theory,[8] the stability analysis is based upon the eigenvalues of the Jacobian matrix. If the real parts of the eigenvalues are negative, then the system of ODEs is said to be stable. If this condition is not met for all the eigenvalues, the associated exponentials in equation (11) grow with time and make the system unbounded. Therefore an inappropriate spatial discretization scheme in the approximation of the convective derivatives may lead to an unstable ODE problem. In order to depict the indispensability of an intelligent scheme, the effect of different spatial discretization schemes on the problem stability is illustrated. This can be carried out by determining the eigenvalues of the Jacobian matrix $[P]$ analytically as

$$\lambda_1 = B + \sqrt{(AC)} - \sqrt{(DE)}, \tag{12a}$$

$$\lambda_2 = B + \sqrt{(AC)} + \sqrt{(DE)}, \tag{12b}$$

$$\lambda_3 = B - \sqrt{(AC)} + \sqrt{(DE)}, \tag{12c}$$

$$\lambda_4 = B - \sqrt{(AC)} - \sqrt{(DE)} \tag{12d}$$

and evaluating them with respect to the differencing scheme and flow direction as follows.

4.4. Case 1: $\bar{\mathrm{u}} > 0, \bar{\mathrm{v}} > 0$*, upwind scheme*

If the velocity components at any point are positive, then the discretization scheme for the approximation of the convective terms should be the upwind scheme. As can be seen from Table I, if the discretization scheme is chosen as upwind, the eigenvalues will then have negative real parts and no imaginary parts. Hence the upwind scheme for the approximation of the convective derivatives for positive velocity components always results in a stable ODE problem.

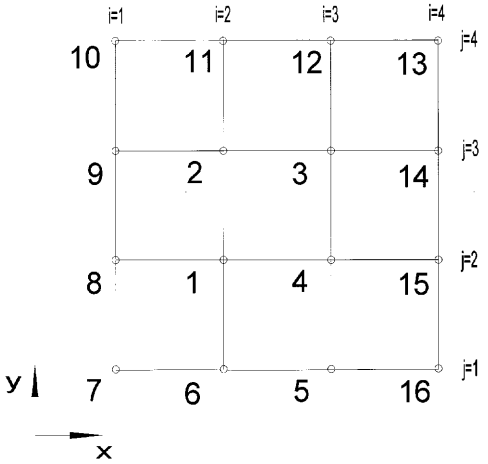

Figure 2. Computational domain for equation (8)

4.5. Case 2: $\bar{u} > 0, \bar{v} > 0$, *downwind scheme*

If the velocity components at any point are positive and the spatial discretization scheme for the approximation of the convective derivatives is downwind, then the eigenvalues will have positive real parts if the mesh Peclet numbers are greater than two; thereby the system of ODEs may become unstable depending on the value of the associated exponentials. Hence the downwind scheme for the approximation of the convective derivatives for positive velocity components is not appropriate from a stability point of view.

4.6. Case 3: $\bar{u} > 0, \bar{v} > 0$, *centred scheme*

If the velocity components at any point are positive and the spatial discretization scheme for the approximation of the convective terms is centred, then the eigenvalues will always have negative real parts, resulting in stability. However, if the mesh Peclet numbers are greater than two, the eigenvalues will have imaginary parts; hence the numerical results exhibit oscillations. This phenomenon is a common characteristic of central differencing schemes.

4.7. Case 4: $\bar{u} < 0, \bar{v} < 0$, *downwind scheme*

In the case of flow reversals the velocity components becomes negative and stability independent of mesh Peclet number can only be obtained if the downwind scheme for the approximation of the convective terms is chosen. Other choices result in an unstable ODE problem, particularly at high Peclet numbers.

5. NUMERICAL SOLUTION TECHNIQUE

5.1. Intelligent higher-order spatial discretization

The instability of the system of ODEs due to an inappropriate spatial discretization scheme can be alleviated by decreasing the value of the mesh Peclet numbers by either decreasing the mesh size or increasing the value of the diffusion coefficient by introducing artificial diffusivity, the former requiring excessive computer storage, the latter being implausible. Therefore in this paper a higher-

order intelligent spatial discretization scheme is proposed. The suggested scheme is based on the fourth-order Lagrange interpolation polynomial.[9,10] If the streamwise component of the velocity at any point (r_i, z_j) is denoted by $u_{i,j}$, the spatial derivatives at the point (r_i, z_j) are approximated by

$$\left.\frac{\partial u}{\partial z}\right|_{i,j} = \sum_{k=-q}^{q} a_{j,m}^{t} u_{i,j+n} = (u_z)_{i,j}, \tag{13a}$$

$$\left.\frac{\partial^2 u}{\partial z^2}\right|_{i,j} = \left.\frac{\partial}{\partial z}(u_z)\right|_{i,j} = \sum_{k=-q}^{q} a_{j,m}^{t} (u_z)_{i,j+n} = (u_{zz})_{i,j}, \tag{13b}$$

where the a's are weighting coefficients, $q = (h-1)/2$, in which h is defined as the order of the Lagrange interpolation polynomial, $m = k + q + 1$ and $n = m - t$, in which t stands for the type of discretization scheme, which is based on one of the five-point grids illustrated in Table II.

For type 1 the spatial derivative of a velocity component, either u or v, at a point I is obtained by interpolating on a Lagrange polynomial that passes through the values of the concerned dependent variable at the four nodes to the right of the point I where the derivative is computed. For type 2 one node to the left and three nodes to the right of the point I where the spatial derivative is computed are used. Type 3 considers two nodes to the left and two nodes to the right of the point I. Types 4 and 5 can be handled similarly.

This procedure is accommodated into the code in a zone-of-dependence manner as follows. The code checks the sign of the coefficient of the convective derivative and decides on the type of discretization scheme as shown in Table II. If the velocity component is positive, type 4 is selected, as the information is carried from the upstream direction. If the velocity component is negative, type 2 is then selected, as the zone of dependence is downstream of the point under consideration. However, for the approximation of the spatial derivatives at the boundary nodes it is not possible to use the same type of scheme as for the interior nodes even if the sign of the velocity component is the same for both the boundary and interior nodes. Therefore either a higher-order scheme at the expense of directionality or directionality at the expense of order is sacrificed for the evaluation of the spatial derivatives at the nodes near the boundaries. In the proposed study a higher-order scheme was utilized at the nodes near the boundary, sacrificing the directionality. Table III summarizes the grid identifiers (discretization types) in a certain direction.

As can be seen from Table III, for the positive velocity component the spatial discretization is type 2 for the boundary node 2. In fact, owing to the directionality, it should have been type 4, which is eventually not possible to use because of fictitious points.

5.2. Treatment of pressure gradient

The comparison of pressure is the most difficult and time-consuming part of the overall solution of the Navier–Stokes equations and there are various pressure correction methods which are applicable to both stationary and time-dependent incompressible flow equations. Basically, most of them

Table II. Types of discretization scheme

Type	Discretization scheme	Grid points to be used				
1	Downwind	I	$I+1$	$I+2$	$I+3$	$I+4$
2	Downwind-biased	$I-1$	I	$I+1$	$I+2$	$I+3$
3	Centred	$I-2$	$I-1$	I	$I+1$	$I+2$
4	Upwind-biased	$I-3$	$I-2$	$I-1$	I	$I+1$
5	Upwind	$I-4$	$I-3$	$I-2$	$I-1$	I

Table III. Summary of grid identifiers for convective derivatives

Grid number:	1	2	3	4	···	$N-4$	$N-3$	$N-2$	$N-1$	N
Grid identifier for positive velocity	1	2	3	4	4	4	4	4	4	5
Grid identifier for negative velocity	1	2	2	2	2	2	2	3	4	5

involve an iterative procedure between the velocity and pressure fields through the solution of Poisson-type equation for the pressure to satisfy the global mass flow constraint and the divergence-free condition for confined incompressible flows. Therefore in this paper a non-iterative procedure proposed recently[11] for the treatment of pressure gradients is applied.

5.3. Time integration

The integration of the resulting ODEs derived from the discretization of the Navier–Stokes equations is carried out by an implicit algorithm (Adams–Moulton) embedded in the well-known ODE solver LSODES.[12] The implicit nature of the solution method requires some additional discussion. In order to illustrate this, a typical implicit formulation for the solution of ODE's can be written in the form of a backward Euler method as

$$\bar{\Omega}^{n+1} = \bar{\Omega}^{n} + \bar{F}(\bar{\Omega}^{n+1})\Delta t, \tag{14}$$

where $\bar{\Omega}^{n+1}$ and $\bar{F}(\bar{Q}^{n+1})$ are the solution and derivative vectors respectively. As can be seen from equation (14), the derivative vector is evaluated at the next time level. In other words, equation (14) is implicit in the derivative vector $\bar{F}(\bar{\Omega}^{n+1})$. It is this implicit term that gives the method its good stability properties. Therefore the elegance of the MOL is that it shares the advantages of both explicit and implicit methods. In the MOL the spatial derivatives and source terms are evaluated at the previous time level as applied in the explicit approach, so that no linearization problem arises. Furthermore, the solution of the resulting ODEs is carried out by an implicit algorithm such as the implicit Adams–Moulton method,[12] backward differentiation formula (BDF) method[12] or implicit Runge–Kutta method.[13] Hence it can be concluded that the MOL has the simplicity of the explicit approach and the power of the implicit one unless a poor algorithm for the solution of ODEs is adapted.

6. NUMERICAL SOLUTION PROCEDURE

The general algorithm for the solution of the Navier–Stokes equations by using the MOL approach is based upon the evaluation of the derivative vector by which the solution is advanced from one time step to the next. Once the derivative vector is obtained, the first step in the solution is to combine the dependent variables into a one-dimensional array. The evaluation of the derivative vector can be summarized as follows.

The complete velocity field satisfying the continuity equation is known *a priori* at the beginning of each cycle either as a result of the previous cycle or from the prescribed initial conditions for the dependent variables. Once the spatial derivatives appearing in the governing equations are evaluated using the initial conditions, the corresponding pressure gradients along the axial direction are calculated in such a way that the mass flow is conserved. Then the radial component of the velocity is calculated by direct utilization of the continuity equation; hence the divergence-free condition is ensured automatically. Once these calculations are settled, the derivative vector is calculated over the spatial domain of interest and then sent to the ODE solver in the form of a one-dimensional array to

compute the dependent variables at the advanced time level. This then completes the progression of the solution to the end of the new cycle, having the new values of the velocity field. This cyclic procedure is then continued until a steady state is reached.

7. FLOW COMPUTATIONS AND RESULTS

The code was run for Reynolds numbers in the range 100–500 on an IBM RISC Sys/6000-590. The distribution of the grid nodes was non-uniform in both radial and axial directions, allowing higher grid node concentrations in the region close to the wall and in the vicinity of the step. The results were found to be independent of grid size beyond 41 and 101 nodes along the radial and axial directions respectively.

Plate 1 shows the time development of the recirculating flow regions, exhibiting both the streamline patterns of the flow and the magnitudes of the axial component of the velocity by colour contours. As can be seen from the figure, as soon as the flow is started, a vortex begins to form in the vicinity of the sudden expansion. Thereafter the flow starts to separate downstream of the step, yielding two disconnected recirculating flow regions. As time progresses, the secondary vortex propagates towards the end of the cylinder and after some time it leaves the system, while the primary recirculating zone attached to the step grows in size. This separated flow region stays attached to the step and continues to grow in size until the steady state flow pattern is reached.

Figure 3 illustrates the variation in the length of the recirculation region at steady state for Reynolds numbers in the range 100–500. As can be seen from the figure, the distance between the step and the point of reattachment on the downstream wall increases linearly with Reynolds number in the range considered. The results of the numerical experiments shown in Plate 1 and Figure 3 agree with the experimental findings of Durst and co-workers.[14,15]

Although it was not possible to validate the present code by comparing its predictions with experimental data owing to the absence of tabulated results in the open literature, the flow field predicted by using this code shows similar behaviour to the unsteady experimental and numerical simulations of impulsively started flows.[14,15]

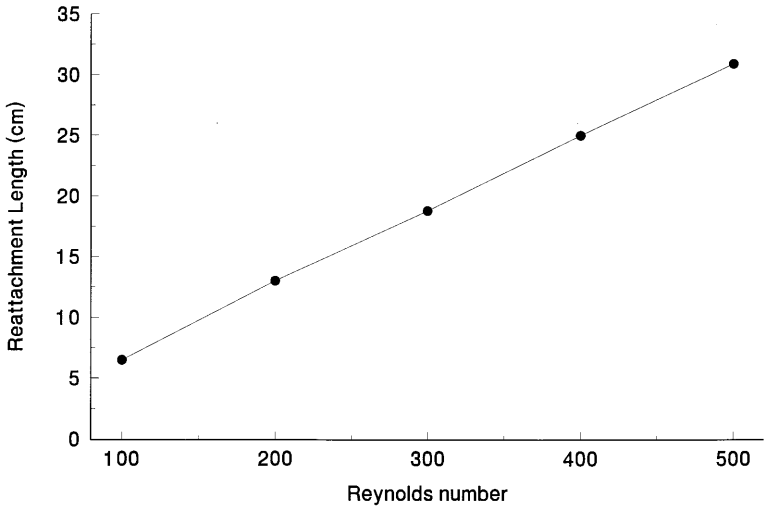

Figure 3. Variation in reattachment length with Reynolds number

8. CONCLUSIONS

The main objective of this study has been to introduce the MOL solution of the time-dependent two-dimensional Navier–Stokes equations for confined separated flows in conjunction with an intelligent higher-order spatial discretization scheme. The computational procedure proposed in this study, namely the MOL, has the simplicity of the explicit approach and the power of the implicit one and does not require any linearization in the governing equations.

Examinations of the stability characteristics of a generic advective–diffusive equation in terms of eigenvalues have shown that an intelligent spatial discretization scheme is indispensable when flow reversal occurs to satisfy the stability of the problem without having any limitations on the mesh Peclet number.

The proposed code has been applied to predict the time development of an impulsively started incompressible flow in a circular pipe with a sudden expansion in the Reynolds number range 100–500. Both transient and stationary predictions were found to be in qualitative agreement with the experimental findings available in the literature.

ACKNOWLEDGEMENT

This study was performed as a part of an AGARD Project T51/PEP on 'Soot formation and radiative heat transfer in combustors'. The support is gratefully acknowledged.

REFERENCES

1. H. O. Kreiss and J. Lorenz, *Initial Boundary Value Problems and the Navier–Stokes Equation*, Academic, San Diego, CA, 1989.
2. R. Temam, *Theory and Numerical Analysis of the Navier–Stokes Equations*, North-Holland, Amsterdam, 1977.
3. F. Thomasset, *Finite Element Methods for Navier–Stokes Equations*, Springer, New York, 1981.
4. R. Glowinski, *Numerical Methods for Non-linear Variational Problems*, Springer, New York, 1984.
5. V. Girault and P. A. Raviart, *Finite Element Methods for Navier–Stokes Equations: Theory and Algorithms*, Springer, Berlin, 1986.
6. V. Patankar, *Numerical Heat Transfer and Fluid Flow*, Hemisphere, Washington, DC, 1980.
7. O. Oymak and N. Selçuk, 'MOL vs FDM solutions of an unsteady viscous flow problem', *Proc. Eighth Int. Conf. on Numerical Methods in Laminar and Turbulent Flows*, Vol. III, Part 1, Pineridge, Swansea, 1993, pp. 151–160.
8. W. E. Schiesser, *The Numerical Method of Lines: Integration of Partial Differential Equations, Academic, San Diego, CA, 1991*.
9. W. E. Schiesser, 'Variable grid spatial differentiator in the numerical method of lines', *DSS/2 Manual No. 6*, Lehigh University, 1988.
10. W. E. Schiesser, *Computational Mathematics in Engineering and Applied Science: ODEs, DAEs, and PDEs*, CRC Press, Boca Raton, FL, 1994.
11. O. Oymak and N. Selçuk, 'Method-of-lines solution of time-dependent two-dimensional Navier–Stokes equations', *Int. j. numer methods fluids*, **23**(5), 455–466 (1996).
12. A. C. Hindmarsh, 'ODEPACK: a systemized collection of ODE solvers', in *Scientific Computing*, North-Holland, New York, 1983.
13. Hairer and G. Wanner, *Solving Ordinary Differential Equations II. Stiff and Differential Algebraic Problems*, Springer, Berlin, 1991.
14. F. Durst and J. C. F. Pereira, 'Time-dependent laminar backward-facing step flow in a two-dimensional duct', *J. Fluids Eng.*, **110**, 289–296 (1988).
15. F. Durst, T. Maxworthy and J. C. F. Pereira, 'Piston-driven, unsteady separation at a sudden expansion in a tube: Flow visualization and LDA measurements', *Phys. Fluids*, **1**, 1249–1260 (1989).

